Talanta 85 (2011) 2344–2351

Contents lists available at ScienceDirect

Talanta

journal homepage: www.elsevier.com/locate/talanta

Selective detection of dopamine in the presence of uric acid using a gold nanoparticles-poly(luminol) hybrid film and multi-walled carbon nanotubes with incorporated β-cyclodextrin modified glassy carbon electrode

Dong Jia[a], Jianyuan Dai[b], Hongyan Yuan[a], Ling Lei[a], Dan Xiao[a,b,*]

[a] College of Chemical Engineering, Sichuan University, Chengdu 610064, PR China
[b] College of Chemistry, Sichuan University, Chengdu 610064, PR China

ARTICLE INFO

Article history:
Received 19 April 2011
Received in revised form 17 July 2011
Accepted 20 July 2011
Available online 27 July 2011

Keywords:
Dopamine
Poly(luminol)
Gold nanoparticles
Multi-walled carbon nanotubes
β-Cyclodextrin

ABSTRACT

Gold nanoparticles-poly(luminol) (Plu-AuNPs) hybrid film and multi-walled carbon nanotubes with incorporated β-cyclodextrin modified glassy carbon electrode (β-CD-MWCNTs/Plu-AuNPs/GCE) was successfully prepared for simultaneous determination of dopamine (DA) and uric acid (UA). The surface of the modified electrode has been characterized by X-ray photo-electron spectroscopy (XPS), energy dispersive X-ray spectroscopy (EDS), field-emission scanning electron microscope (SEM) and transmission electron microscope (TEM). Cyclic voltammetry (CV), electrochemical impedance spectroscopy (EIS) and differential pulse voltammetry (DPV) have been used to investigate the β-CD-MWCNTs/Plu-AuNPs composite film. Gold nanoparticles anchored into poly(luminol) film exhibited catalytic activity for DA. MWCNTs with incorporated β-CD can greatly promote the direct electron transfer. In 0.10 M phosphate buffer solution (PBS, pH 7.0), the DPV response of the β-CD-MWCNTs/Plu-AuNPs/GCE sensor to DA is about 8-fold as compared with the Plu-AuNPs/GCE sensor, and the detection limit for DA is about one order of magnitude lower than the Plu-AuNPs/GCE sensor. The steady-state current response increases linearly with DA concentration from 1.0×10^{-6} to 5.6×10^{-5} M with a low detection limit ($S/N = 3$) of 1.9×10^{-7} M. Moreover, the interferences of ascorbic acid (AA) and uric acid (UA) are effectively diminished. The applicability of the prepared electrode has been demonstrated by measuring DA contents in dopamine hydrochloride injection.

1. Introduction

Dopamine (DA) is one of the important catecholamine neurotransmitters in the mammalian central nervous system, and is related to the pathological and physiological process of Parkinson's disease [1]. Therefore, it is of great significance to quantify the content of DA in human body fluids. Electrochemical method had been applied to detect DA for a long time. However, the fouling of electrode surface by the oxidation product can result in poor performance at the conventional electrodes. Furthermore, the coexisted uric acid (UA) and ascorbic acid (AA) in the body fluids in high levels can be easily oxidized at a potential rather close to that of DA and always interfere with the determination of DA at the conventional electrodes. Thus, selective determination of DA in the coexisted UA and AA is significant and various modified electrodes have been proposed to determine the content of DA by their electrocatalytic activity, such as polymer film modified electrode [2–9], metal complex with electroactive center modified electrode [10–16], carbon based materials [17–24] and composites based on the above materials [19,25–30]. Kumar et al. proposed the poly(luminol) film to discriminate UA from DA with good selectivity [31]. However, the poor electrical conductivity may degrade the sensitivity and detection limit. Therefore, the development of high conductivity materials with simple preparation method for sensitive simultaneous determination of DA and UA is still attractive in the electrochemical field.

In this work, gold nanoparticles-poly(luminol) hybrid film and multi-walled carbon nanotubes with incorporated β-cyclodextrin were explored to modify glassy carbon electrode. Poly(luminol) film entrapped gold nanoparticles have the probable electronic interactions. The porous structure of poly(luminol) film allows the gold nanoparticles dispersing into the polymer matrix and generates additional electrocatalytic sites. Carbon nanotubes (CNTs) can facilitate electron transfer between the electroactive species and electrode, and β-CD is used as a dispersing reagent for carbon nanotubes. When applied to simultaneous determination of DA and UA, the β-CD-MWCNTs/Plu-AuNPs/GCE exhibited good selectivity and sensitivity with well-separated DPV peaks. Low

* Corresponding author. Tel.: +86 28 85415029; fax: +86 28 85416029.
E-mail address: xiaodan@scu.edu.cn (D. Xiao).

0039-9140/$ – see front matter © 2011 Elsevier B.V. All rights reserved.
doi:10.1016/j.talanta.2011.07.067

detection limits for all these species were obtained due to the high electrocatalytic properties of the β-CD-MWCNTs/Plu-AuNPs film. Interference from AA and UA was efficiently eliminated and analytical applications such as real sample analysis are also investigated.

2. Experimental

2.1. Materials and reagents

MWCNTs were obtained from Chengdu Organic Chemicals Co. Ltd. (Chengdu, China). β-cyclodextrin (β-CD) was provided by Kermel Chemical Reagent Company (Tianjin, China) and L-ascorbic acid (AA) was purchased from Kelong Chemical Reagent Company (Chengdu, China). Dopamine hydrochloride (DA) and uric acid (UA) were obtained from Alfa Aesar (A Johnson Matthey Co., Tianjin, China). Luminol was obtained from Sigma Aldrich Fluka (Buchs, Switzerland), Hydrogen tetrachloroaurate (III) trihydrate ($HAuCl_4 \cdot 3H_2O$, +99.9%) was obtained from Sigma Aldrich (Milwaukee, WI, USA). Other reagents were of analytical grade and used as received. Measurements were carried out in pH 7.0 phosphate buffer solution (PBS) at room temperature under nitrogen atmosphere.

2.2. Instrumentation

Cyclic voltammetry (CV) and differential pulse voltammetry (DPV) were performed using a potentiostat/galvanostat Auto lab (PGSTAT 30/302, Netherlands) electrochemical analyzer system. A three-electrode configuration was employed, consisting of a bare or modified GCE (Ø3 mm, LANLIKE, Tianjin, China) as a working electrode, a saturated calomel as reference electrode (SCE) and a Pt flake auxiliary electrode. The surface morphology of modified electrode was analyzed by field-emission scanning electron microscopy (SEM, Hitachi S-4800, Tokyo, Japan) and transmission electron microscope (TEM, JEM 100CX II, Japan). The chemical composition of the material was analyzed by energy dispersive X-ray (EDS, Hitachi S-4000, Tokyo, Japan) and X-ray photoelectron spectroscopy (XPS, Kratos, XSAM 800).

2.3. Preparation of the β-CD-MWCNTs/Plu-AuNPs/GCE

A bare GCE was polished carefully to a mirrorlike surface with 1.0–0.05 μm alumina slurry and then rinsed with double distilled water, and sonicated in ethanol and double distilled water for 5 min, respectively. Prior to the electrochemical deposition of poly(luminol)-AuNPs, the bare GCE was cyclic-potential scanned firstly in the potential range from −0.10 to 1.0 V in 0.50 M H_2SO_4 for activating the electrode and then from −0.20 to +0.60 V in 5.0 mM $Fe(CN)_6^{3-/4-}$ solution containing 0.10 M KCl supporting electrolyte until a pair of well-defined redox peaks was observed. Finally, the electrode was immersed in 1.0 mM luminol and 0.10 M H_2SO_4 solution containing 2.0×10^{-4} M $HAuCl_4$ and treated by using cyclic voltammetry between −0.10–1.0 V for 30 cycles (Fig. S1, Supplementary Material). Thus, the Poly(luminol)-AuNPs-GC electrode (denoted as Plu-AuNPs/GCE) was obtained. MWCNTs were treated according to Ref. [32]. 1.0 mg functionalized MWCNTs were dispersed with the aid of ultrasonic agitation in 1.0 mL aqueous β-CD solution (1.0%) to give a 1.0 mg mL^{-1} black suspension. 6.0 μL β-CD-MWCNTs dispersion were scrupulously dropped onto the surfaces of Plu-AuNPs/GCE. After evaporation of solvent in air at the room temperature overnight, the β-CD-MWCNTs/Plu-AuNPs/GCE was achieved (Fig. 1A).

2.4. Electrochemical measurements

Before electrochemical measurements, the β-CD-MWCNTs/Plu-AuNPs/GCE was treated in pH 7.0 PBS by repetitive scanning in the potential range of −0.10 and +0.40 V for 20 cycles at a scan rate of 50 mV s^{-1} until a stable background was obtained. DPV was recorded in the range of −0.20–0.50 V at the same scan rate with the pulse amplitude: 25 mV; pulse rate: 0.5 s; pulse width: 60 ms, respectively. The EIS was scanned in 5.0 mM $Fe(CN)_6^{3-/4-}$ and 0.10 M KCl solution at the formal potential of 0.00 V with the frequency range between 0.01 and 1.0×10^5 Hz (signal amplitude: 10 mV).

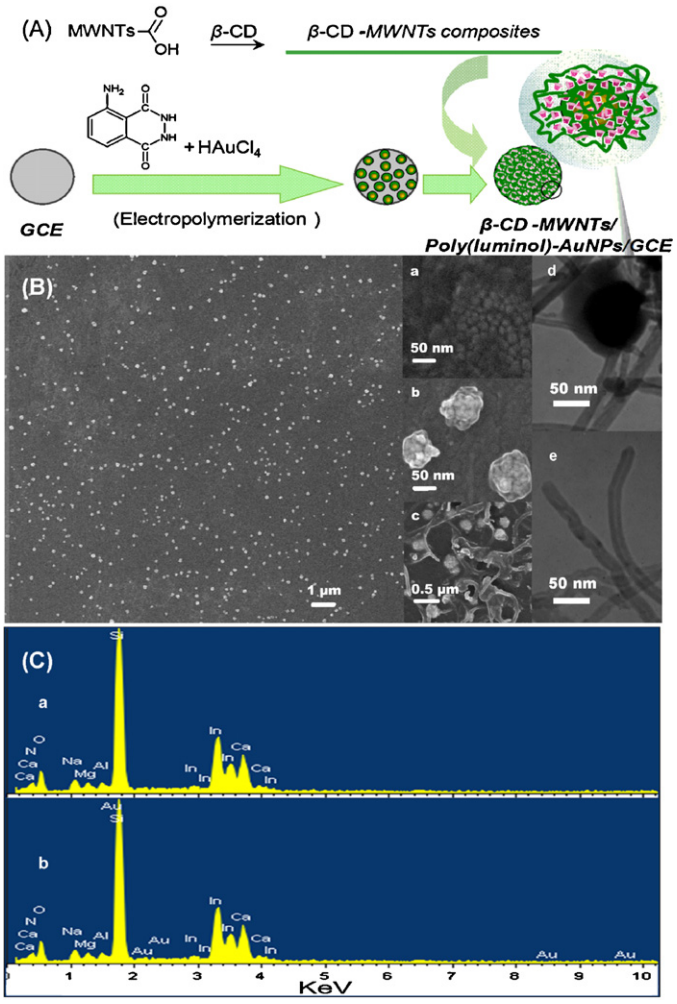

Fig. 1. (A) The preparation procedures of β-CD-MWCNTs/Plu-AuNPs/GCE. (B) Typical SEM image of the poly(luminol)-AuNPs film on the ITO electrode surface (inset shows the SEM image of poly(luminol) film (a), Plu-AuNPs film (b), β-CD-MWCNTs/Plu-AuNPs film (c), and TEM image of β-CD-MWCNTs/Plu-AuNPs (d) and β-CD-MWCNTs (e)). (C) EDS spectra of Poly(luminol) film (a) and Plu-AuNPs film (b) on ITO electrode.

3. Results and discussion

3.1. SEM, TEM, EDS and XPS analysis

SEM and TEM images of Plu-AuNPs film and β-CD-MWCNTs/Plu-AuNPs film are shown in Fig. 1B. The electrode surface was covered by a Plu-AuNPs film and the AuNPs have an average size of about 80–100 nm. Inset (a) shows morphology feature of poly(luminol) film. As shown in the inset (b), the AuNPs were embedded in the poly(luminol) film matrix and wrapped partially by poly(luminol) to form the core-shell structure, which was more clearly demonstrated by the TEM characterization (inset (d)). The surface of the β-CD-MWCNTs/Plu-AuNPs film was depicted in inset (c). Homogeneous MWCNTs could be observed

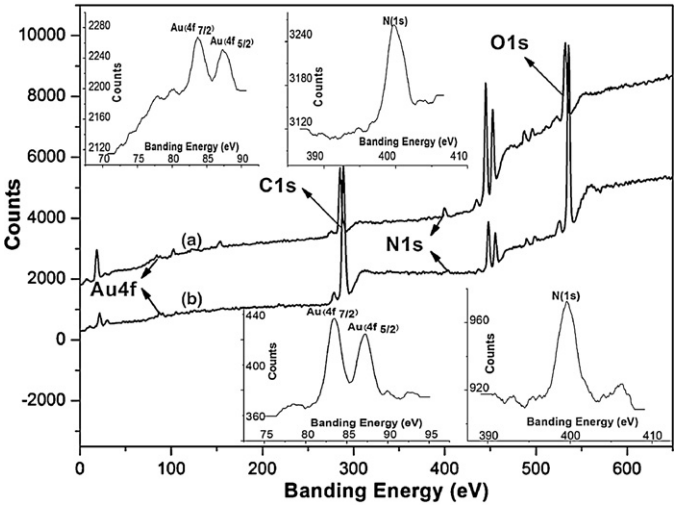

Fig. 2. XPS spectra of Plu-AuNPs film (a) and β-CD-MWCNTs/Plu-AuNPs film (b) on ITO electrode. Inset shows the high-resolution spectra of N (1s) peak and Au ($4f_{7/2}$) and Au ($4f_{5/2}$) double peaks.

clearly in perspective and the AuNPs relatively evenly distributed under the MWCNTs. Inset (e) shows the morphology feature of β-CD-MWCNTs with a diameter of about 20 nm. As shown in Fig. 1C, the level of nitrogen was detected for poly(luminol) film (19.53, Atomic %) and no Au element was found in EDS analysis (Fig. 1C(a)), only lower level of gold was detected for Plu-AuNPs film (0.05, Atomic %) in Fig. 1C(b). However, XPS results proved the existence of Au in the Plu-AuNPs film (Fig. 2(a)) and β-CD-MWCNTs/Plu-AuNPs film (Fig. 2(b)). The position of N (1s) peak maximum (399.93 eV, 5.01%) is consistent with the formation of carbon–nitrogen bond between the amine cation radical and a luminol molecular. The high-resolution spectra shows clearly the peaks of Au (4f) at 83.78 eV and 87.44 eV (0.32%).

3.2. Characterization of the modified electrode interface with cyclic voltammetry and electrochemical impedance spectroscopy (EIS)

Fig. 3A shows the cyclic voltammograms responses of 5.0 mM $Fe(CN)_6^{3-/4-}$ and 0.10 M KCl at the bare GCE, Plu-AuNPs/GCE and β-CD-MWCNTs/Plu-AuNPs/GCE, respectively. The CV curve of the bare GCE showed a pair of quasi-reversible peaks (Fig. 3A, curve a). The redox peak current decreased obviously after the Plu-AuNPs deposition onto the bare GCE surface (Fig. 3A, curve b), which can be attributed to the poor electrical conductivity of Poly(luminol) film. When β-CD-MWCNTs were attached to the Plu-AuNPs film-coated electrode surface, a pair of redox peaks was recorded as shown in Fig. 3A, curve c, it can be found that the voltammetric response of $Fe(CN)_6^{3-/4-}$ is evidently restored.

On the other hand, the EIS has been employed to investigate the impedance changes of the electrode surface, which is an effective method for probing the features of a surface-modified electrode. The semicircle portion at high frequencies corresponds to the electron-transfer limited process and the linear portion at low frequencies may be attributed to diffusion. Curves a and c in Fig. 3B displays the EIS of the bare GCE and β-CD-MWCNTs/Plu-AuNPs/GCE, respectively. The semicircle diameter shows the electron-transfer resistance (R_{ct}), which depends on the insulating and dielectric features between the electrode and electrolyte interface [33–35]. The straight lines were characteristic of a mass diffusion limiting electron-transfer process [36,37]. The Randle's equivalent circuit (inset of Fig. 3B, top) could help to understand clearly the electrical properties of the electrodes/solution interfaces, and it was chose to fit the obtained impedance data [38,39]. It was assumed that the diffusion impedance (W) and the resistance to charge transfer (R_{ct}) were both in parallel to the interfacial capacity (C_{dl}). In the complex plane plot of Z'' against Z', this parallel combination of R_{ct} and C_{dl} can give rise to a semicircle. This resistance exhibits the faster electron-transfer kinetics of $Fe(CN)_6^{3-/4-}$ on the bare GCE and β-CD-MWCNTs/Plu-AuNPs/GCE, there is a very low charge transfer resistance for the electrode (Fig. 3B, curves a and c). However, after the Plu-AuNPs were electrodeposited onto the bare GCE surface, the R_{ct} increases dramatically to about 65.7 kΩ (Fig. 3B, curve b), these results indicate the Plu-AuNPs film has the larger obstruction effect, which hinders the charge transfer and results in reducing electron-transfer rate or increasing resistance to the flow of electrons (Inset (top) is the Randle's equivalent circuit). When β-CD-MWCNTs were dropped on Plu-AuNPs/GCE surface, the R_{ct} decreases to low levels (Fig. 3B, curve *c*). It indicates that β-CD-MWCNTs play a role similar to a conductive metal wire to make the electron transfer easier [40,41]. It is consistent with the cyclic voltammetry results above.

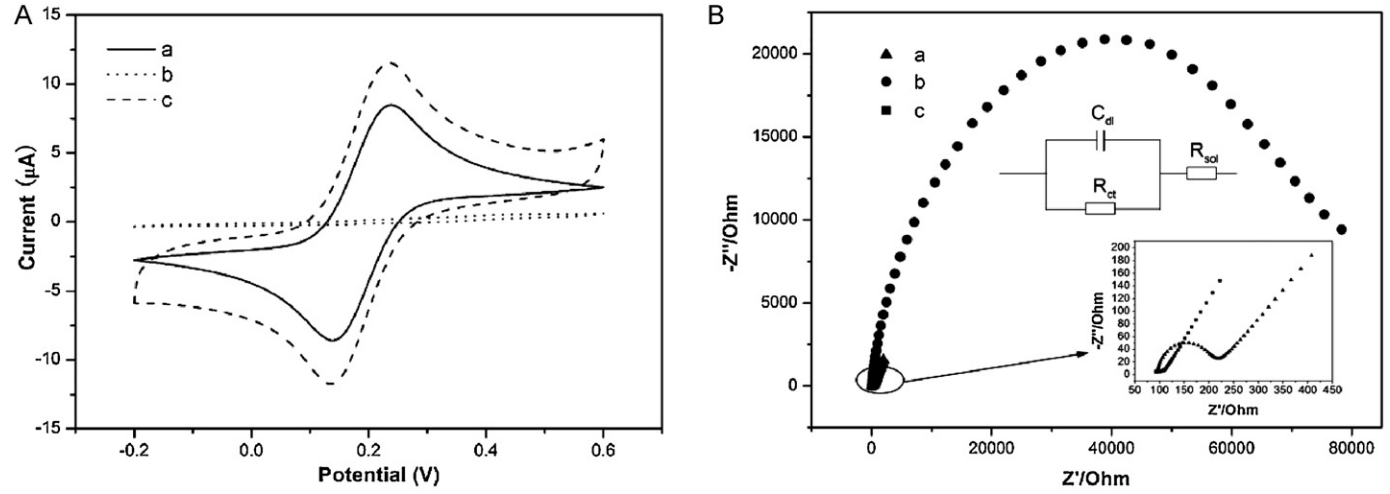

Fig. 3. Cyclic voltammograms (A) and electrochemical impedance spectra (B) of the bare GCE (a), Plu-AuNPs/GCE (b), and β-CD-MWCNTs/Plu-AuNPs/GCE (c) in 5.0 mM $Fe(CN)_6^{3-/4-}$ solution containing 0.10 M KCl supporting electrolyte. Scan rate: 50 mV s^{-1}. Inset (B) displays the Randle's equivalent circuit.

3.3. The possible redox reaction process of luminol's polymerization

The possible chemical changes of a poly(luminol) film undergoing a redox process is as shown in Scheme 1. The free radical which is produced from the oxidation of amino group in the top is essential to form the polymer. It is presumed that all of the luminol oligomers are formed via a series of oxidation/addition reactions starting with the oxidation of luminol to the radical cation, and followed by radical-radical coupling to form the head-to-tail, tail-to-tail, and/or the head-to-head dimer (2-mer). Then the dimers are oxidized to larger n-mers by a series of proton/electron elimination/addition (steps A–C in Scheme 1). The steps B and C are similar to the polymerizing process of aniline, which may be the

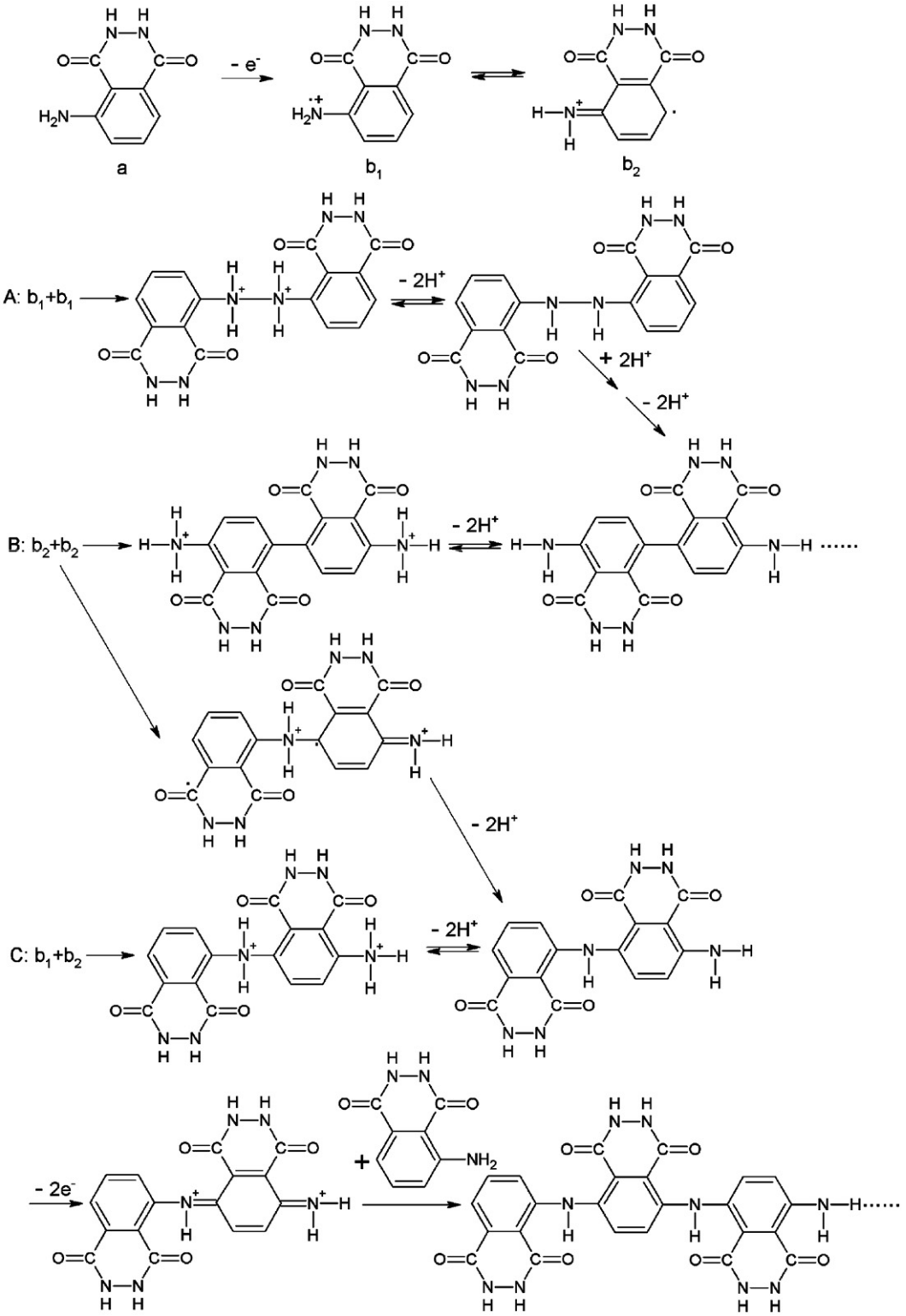

Scheme 1. Redox reaction process of luminol's polymerization.

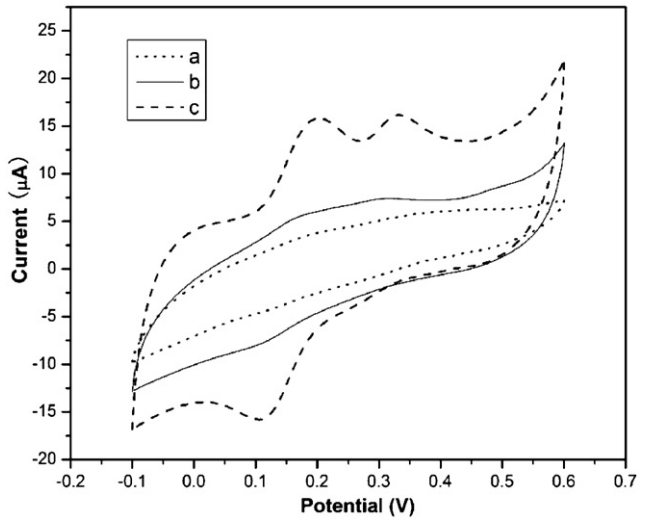

Fig. 4. Cyclic voltammograms of 25 μM DA and 60 μM UA at (a) bare GCE; (b) Plu-AuNPs/GCE and (c) β-CD-MWCNTs/Plu-AuNPs/GCE in phosphate buffer (pH 7.0). Scan rate: 50 mV s^{-1}.

major dimeric product of luminol electropolymerization in acidic aqueous solution [42,43].

3.4. The possible reaction mechanism for the redox process of DA

Fig. 4 shows the cyclic voltammograms of bare GCE (a), Plu-AuNPs/GCE (b) and β-CD-MWCNTs/Plu-AuNPs/GCE (c) in phosphate buffer (pH 7.0) containing 25 μM DA and 60 μM UA. It can be seen there is no obvious electrochemical response at bare GCE and Plu-AuNPs/GCE for DA and UA, while β-CD-MWCNTs/Plu-AuNPs/GCE leads to a pair of well-defined redox peaks at the oxidation potentials of 0.20 V and 0.33 V, respectively. It exhibits that β-CD-MWCNTs do play an important role as an efficient electro-conducting tunnel. On the other hand, due to the high ratio of surface to volume of β-CD-MWCNTs, this modified electrode shows a better current response to DA (Fig. 4). A reversible electron transfer process with the multiples of the same proton exchange process is shown in Scheme 2. DA was oxidized to intermediate material after a closed-loop reaction [44], however, it cannot be achieved the ring closure reaction in the acid solution.

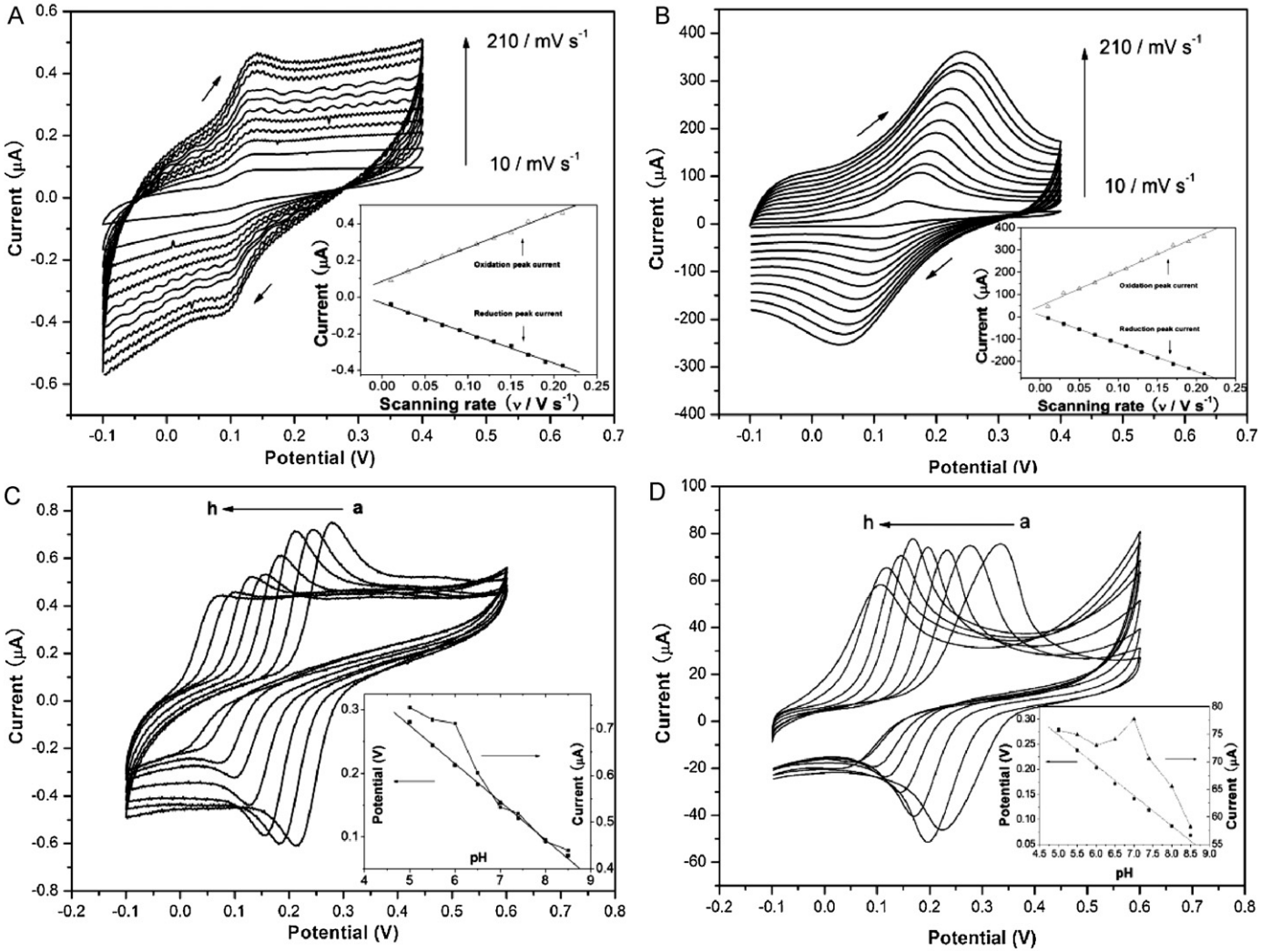

Fig. 5. Cyclic voltammograms of bare GCE (A) and β-CD-MWCNTs/Plu-AuNPs/GCE (B) in 0.10 M pH 7.0 PBS at different scan rates. The scan rates from inner to outer are 0.01, 0.03, 0.05, 0.07, 0.09, 0.11, 0.13, 0.15, 0.17, 0.19, 0.21 V s^{-1}, respectively. Inset is the plot of cathodic and anodic peak currents versus scan rates. Cyclic voltammetric response of the bare GCE (C) and β-CD-MWCNTs/Plu-AuNPs/GCE (D) to 1.0 mM DA in 0.10 M PBS of different pH: (a) pH 5.0, (b) pH 5.5, (c) pH 6.0, (d) pH 6.5, (e) pH 7.0, (f) pH 7.4, (g) pH 8.0, (h) pH 8.5. Scan rate: 50 mV s^{-1}. Inset: plots of peak potential for DA and anodic peak current against pH.

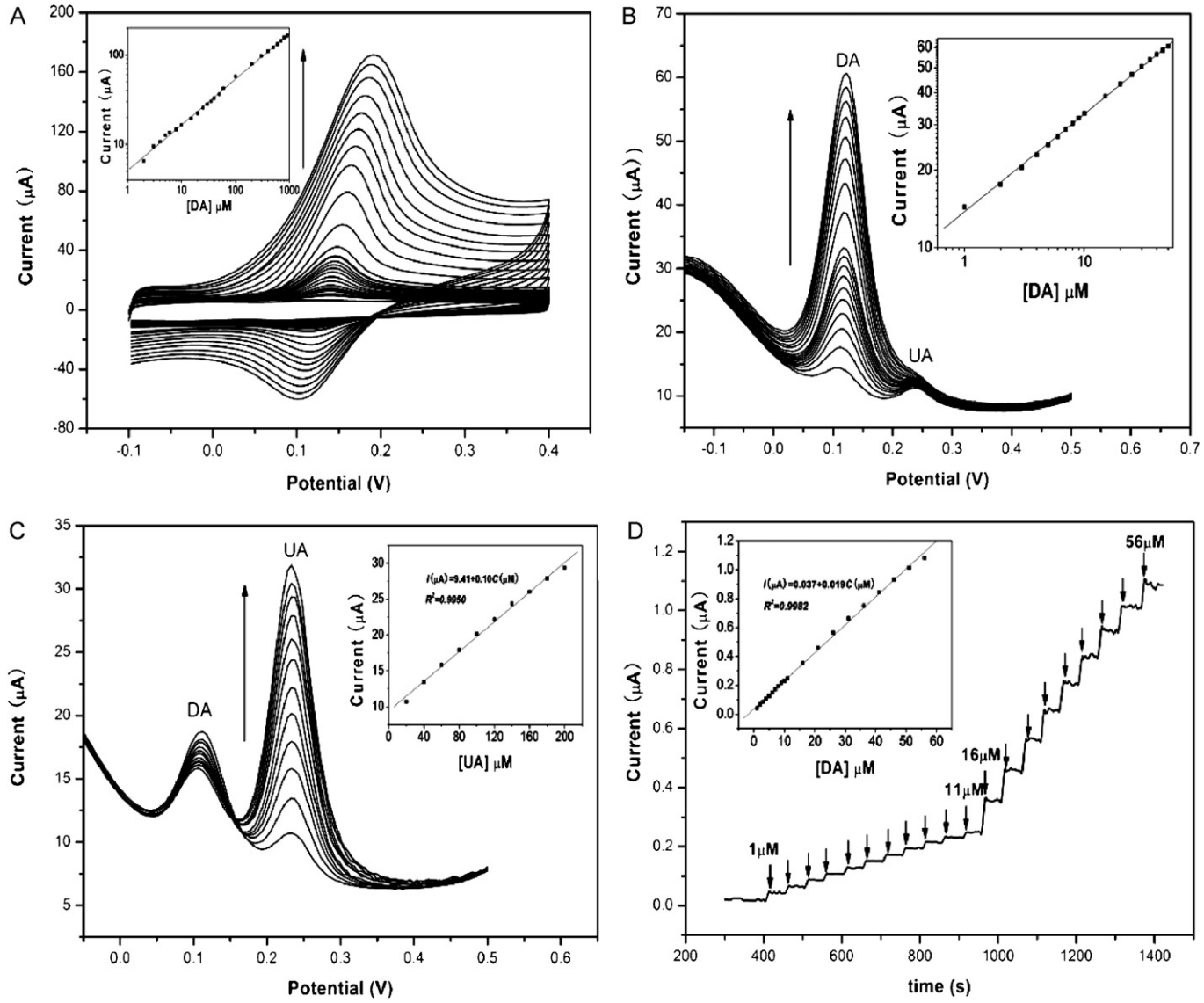

Fig. 6. (A) Cyclic voltammograms obtained from the β-CD-MWCNTs/Plu-AuNPs/GCE for different concentrations of DA (5, 10, 15, 20, 25, 30, 40, 45, 55–1000 μM) in 0.10 M PBS (pH 7.0). Scan rate: 50 mV s^{-1}. (B) DPVs of 15 μM UA in the different concentrations of DA (1–10, 15, 20, 25, 30, 35, 40, 45 and 50 μM) and (C) DPVs of 5 μM DA in the different concentrations of UA (20, 40, 60, 80, 100, 120, 140, 160, 180, 200, 220 and 240 μM) at β-CD-MWCNTs/Plu-AuNPs/GCE in PBS (pH 7.0). (D) Current–time curves for β-CD-MWCNTs/Plu-AuNPs/GCE at 0.161 V with successive addition of DA. Arrow shows the concentrations of DA added in solution. All inset shows its corresponding calibration curve.

3.5. Effect of the scan rate and solution pH

Fig. 5A and B show the cyclic voltammograms of bare GCE and β-CD-MWCNTs/Plu-AuNPs/GCE in 0.10 M pH 7.0 PBS containing 45 μM DA at different scan rates. It can be seen that the I_p increases linearly with scan rates (inset of Fig. 5A and B), indicating that the pair of redox waves of bare GCE and modified electrode both originate from the surface confined molecules. Meanwhile, the peak current at the bare GCE with a lot of noise is much lower than that at the modified electrode. The linear regression equations of modified electrode were I_{pa} (μA) = 48.54 + 1544.22 ν (V s^{-1}) and I_{pc} (μA) = 7.39 − 1258.92 ν (V s^{-1}) with the correlation coefficients (r^2) of 0.993 and 0.999, respectively.

To investigate the improved electroactivity of the β-CD-MWCNTs/Plu-AuNPs/GCE, the CVs of bare GCE and the modified GCE in solutions with different pH-values have been illustrated (Fig. 5C and D). The results indicate that bare GCE and the β-CD-MWCNTs/Plu-AuNPs/GCE show nearly fewer redox activity in media with pH ≥ 8.5. When pH of the solution is 7.0, the modified electrode shows the maximum peak current while the bare GCE shows lower response to DA in this pH value. It was found that the anodic peak potential shifted negatively with increasing pH of the solution, suggesting that protons participated in the electrode reaction. In this study, the oxidation process of DA involves the transfer of two protons and two electrons. The relationship between the peak potential and pH could be expressed by the equation E_p = 0.574–0.060 pH (bare GCE) and E_p = 0.570–0.060 pH (modified electrode) with the correlation coefficient (r^2) of 0.998 and 0.990, respectively. The E_p was estimated from the average value of anodic and cathodic peak potentials (($E_{pa} + E_{pc}$)/2). The gradient was −60 mV/pH, a value close to that expected from calculations using the Nernst equation. This phenomenon indicates that the uptake of electrons is accompanied by the same protons. Hence, 0.10 M PBS (pH 7.0) was selected for further electrochemical investigation of DA at β-CD-MWCNTs/Plu-AuNPs/GCE.

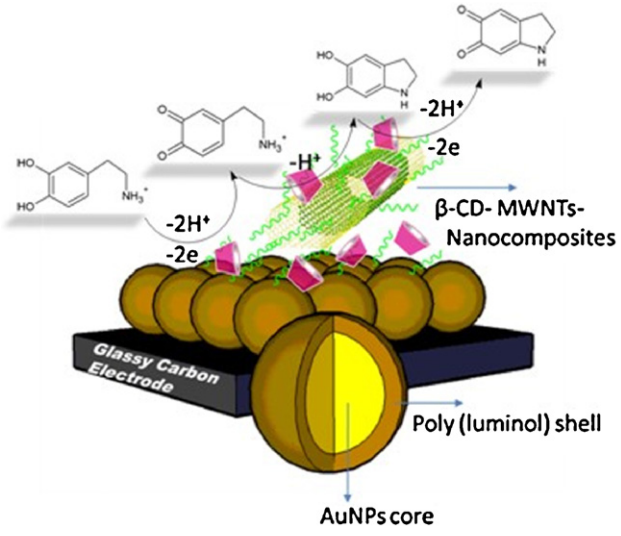

Scheme 2. The possible reaction mechanism for the redox process of DA.

3.6. Electrochemical behavior of DA and UA at the β-CD-MWCNTs/Plu-AuNPs/GCE

Fig. 6A shows the cyclic voltammograms of different concentrations of DA. The redox peaks on the β-CD-MWCNTs/Plu-AuNPs/GCE are much narrower and give only a small increase in ΔE_p even if the DA concentration increased to 1.0 mM, revealing a more reversible electrochemical redox reaction. Calibration curves of the β-CD-MWCNTs/Plu-AuNPs/GCE shows that the logarithm of anodic peak current ($\log I_{pa}$) versus the logarithm of DA concentration curve has a linear range of 5.0×10^{-6} M to 1.0×10^{-3} M. The detection limit was 1.9×10^{-7} M ($S/N = 3$), one order of magnitude lower than that of the poly(luminol)/GCE [31]. The applicability of the β-CD-MWCNTs/Plu-AuNPs/GCE to the simultaneous determination of DA and UA was demonstrated as shown in Fig. 6B and C. The results indicate that the logarithm of peak current ($\log I_p$) response for the oxidation of DA increases linearly with the increase of the logarithm of DA concentration in the range of 1.0×10^{-6} M to 5.0×10^{-5} M, while the peak current for UA oxidation keeps nearly unchanged. The detection limit ($S/N = 3$) is 3.8×10^{-7} M. Similarly, it can be seen that, with increasing of UA concentration, the oxidation current of UA exhibits a linear increase, while the peak response of DA keeps almost stable. The detection limit ($S/N = 3$) is 6.8×10^{-7} M. This indicates that DA and UA do not interfere with each other, and thus the proposed method can be used for the simultaneous determination of DA and UA.

Fig. 6D shows the amperometric responses of β-CD-MWCNTs/Plu-AuNPs/GCE for DA detection at an applied potential of 0.161 V. It showed linear response for DA determination from 1.0×10^{-6} M to 5.6×10^{-5} M and the detection limit was 1.9×10^{-7} M ($S/N = 3$). After the addition of DA, the β-CD-MWCNTs/Plu-AuNPs/GCE need about 1.5 s to reach the steady-state current, it is clear that the response to DA is largely improved.

3.7. Interference study

Interference from AA and UA was studied. The DPV of 45 μM AA, 15 μM DA and 45 μM UA mixtures in PBS (pH 7.0) shows well defined anodic peaks at −10, 122 and 253 mV, respectively. The oxidation of AA and UA does not influence the current response of DA (Fig. 7A). Interference of the β-CD-MWCNTs/Plu-AuNPs/GCE to DA was studied by calculating the ratio of peak current (I_s/I_0). I_s and I_0 were DPV peak current of DA at 122 mV in the present

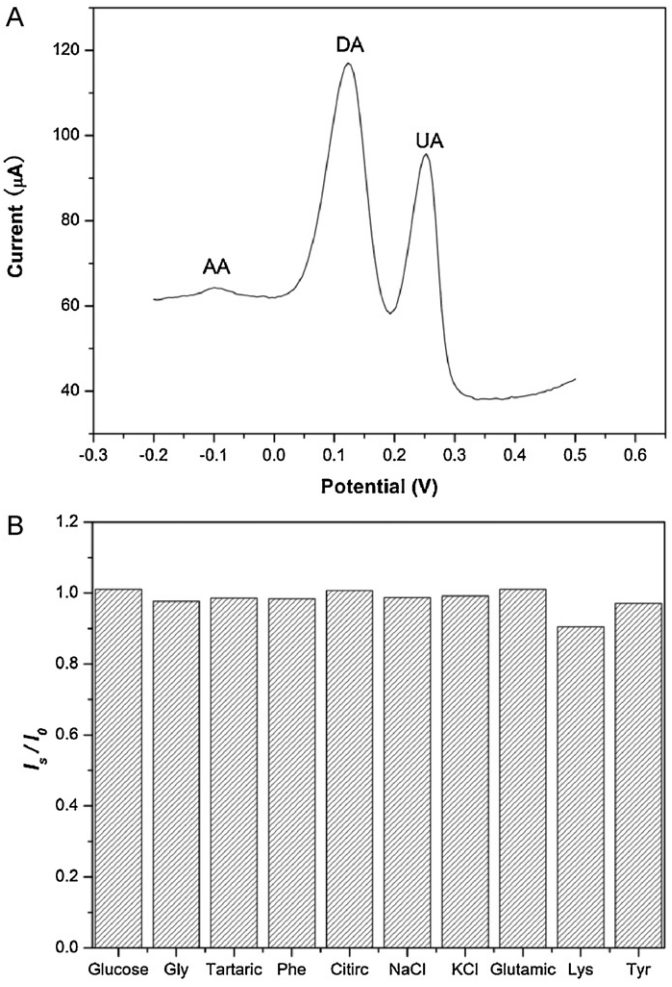

Fig. 7. (A) DPV of 45 μM AA, 15 μM DA and 45 μM UA mixtures at β-CD-MWCNTs/Plu-AuNPs/GCE in phosphate buffer (pH 7.0). (B) Anodic peak current ratio (I_s/I_0) of the β-CD-MWCNTs/Plu-AuNPs/GCE to 12 μM DA in the presence of glucose (200), glutamic acid (200), citric acid (100), tyrosine (200), phenylalanine (200), tartaric acid (100), glycine (200), lysine (200), NaCl (500), KCl (500), respectively.

and absence of other compounds, it hardly causes the significant change of peak current of DA (Fig. 7B). Peak current ratio only slightly varied from 0.91 to 1.01 in the presence of some possible interfering substances including glucose (200), glutamic acid (200), citric acid (100), tyrosine (Tyr, 200), phenylalanine (Phe, 200), tartaric acid (100), glycine (Gly, 200), lysine (Lys, 200), NaCl (500), KCl (500), respectively (where the data in the brackets were the concentration ratios). These results indicate that selective and sensitive determination of DA is possible at β-CD-MWCNTs/Plu-AuNPs/GCE.

3.8. Reproducibility and stability

A series of repetitive measurements were carried out in 25 μM DA solutions to characterize the reproducibility of this sensor. The electrode can be cleaned with voltammetric cycles from −0.10 to 0.40 V for 20 cycles in pH 7.0 PBS to eliminate the adsorption and stored at 4 °C after each determination. The results of 11 successive measurements show a relative standard deviation of 2.8%, indicating that the modified electrode had excellent reproducibility and ability to prevent the electrode from fouling by the oxidation product. The stability of the sensor was also determined. When the electrode was stored in pH 7.0 PBS, the current response signal decreased about 6.0% of its initial response during the first 3 days and about 10% in the next 2 weeks. β-CD-MWCNTs/Plu-AuNPs/GCE

Table 1
The results for the determination of DA in dopamine hydrochloride injection.

No.	DA in dopamine hydrochloride injection						
	Content (μM)	Found (μM)	R.S.D. (%) (n = 5)	Spiked (μM)	Found (μM)	R.S.D. (%) (n = 5)	Recovery (%)
1	5.30	5.17	2.1	2.00	1.92	2.5	96.0
2	5.30	5.22	3.0	4.00	3.95	2.4	98.8
3	5.30	5.20	2.8	6.00	5.74	3.6	95.7

retains 85% of its original activity after a month and continued to exhibit excellent response to DA. The stability of this modified electrode is relatively satisfactory.

3.9. Determination of DA in real samples

Finally, to verify its workability, the sensor was applied to the determination of DA in dopamine hydrochloride injection. Dopamine hydrochloride injection solution (concentration of DA 10 mg mL^{-1}, 2.0 mL per injection) was diluted to 5.30 μM with PBS (pH 7.0). 50 mL of this diluted solutions as the standard DA solutions were injected into each of a series of 100 mL volume flasks. This proposed electrode system gave rise to a better recovery for the determination of spiked DA using DPV method. The results are listed in Table 1.

4. Conclusion

The study has proved that using the bioactive species β-CD-MWCNTs/Plu-AuNPs for surface modification is advantageous for biosensors of dopamine and uric acid. Indeed, β-CD-MWCNTs/Plu-AuNPs showed good electrocatalytic activity for the oxidation. The proposed method can be applied for their determination in a mixture sample with satisfactory results. The DPV response of the modified electrode is about 8-fold compared to that of the Plu-AuNPs/GCE with a lower detection limit for DA. The good selectivity and high sensitivity of the β-CD-MWCNTs/Plu-AuNPs/GCE make it a promising candidate for biomedical application.

Acknowledgements

We sincerely thank Dr. Yi He at the Analytical & Testing Center of Sichuan University for the Measurement of TEM. Financial supports from the National Nature Science Foundation of China (No. 20775050, No. 20927007 and No. 21005051) are gratefully acknowledged.

Appendix A. Supplementary data

Supplementary data associated with this article can be found, in the online version, at doi:10.1016/j.talanta.2011.07.067.

References

[1] J.W. Mo, B. Ogorevc, Anal. Chem. 73 (2001) 1196–1202.
[2] X.M. Cao, Y.H. Xu, L.Q. Luo, Y.P. Ding, Y. Zhang, J. Solid State Electrochem. 14 (2010) 829–834.
[3] W. Song, Y. Chen, J.A. Xu, X.R. Yang, D.B. Tian, J. Solid State Electrochem. 14 (2010) 1909–1914.
[4] X.Y. Wang, F. Yin, Y.F. Tu, Anal. Lett. 43 (2010) 1507–1515.
[5] N.F. Atta, A. Galal, R.A. Ahmed, Bioelectrochemistry 80 (2011) 132–141.
[6] J.H. Chen, J. Zhang, X.H. Lin, H.Y. Wan, S.B. Zhang, Electroanalysis 19 (2007) 612–615.
[7] P. Kalimuthu, S.A. John, Bioelectrochemistry 77 (2009) 13–18.
[8] H.S. Wang, T.H. Li, W.L. Jia, H.Y. Xu, Biosens. Bioelectron. 22 (2006) 664–669.
[9] K. Jackowska, J. Maciejewska, K. Pisarek, I. Bartosiewicz, P. Krysinski, A.T. Biegunski, Electrochim. Acta 56 (2011) 3700–3706.
[10] M.S.C. Lu, Y.C. Chen, P.C. Huang, Biosens. Bioelectron. 26 (2010) 1093–1097.
[11] J.B. Raoof, A. Kiani, R. Ojani, R. Valiollahi, S. Rashid-Nadimi, J. Solid State Electrochem. 14 (2010) 1171–1176.
[12] R.M.A. Tehrani, S. Ab Ghani, Sens. Actuators B 145 (2010) 20–24.
[13] J.W. Choi, W.A. El-Said, J.H. Lee, B.K. Oh, Electrochem. Commun. 12 (2010) 1756–1759.
[14] S. Thiagarajan, S.M. Chen, Talanta 74 (2007) 212–222.
[15] W.A. El-Said, J.-H. Lee, B.-K. Oh, J.-W. Choi, Electrochem. Commun. 12 (2010) 1756–1759.
[16] T.C. Wen, C.Y. Li, Y.J. Cai, C.H. Yang, C.H. Wu, Y. Wei, T.L. Wang, Y.T. Shieh, W.C. Lin, W.J. Chen, Electrochim. Acta 56 (2011) 1955–1959.
[17] S.F. Hou, M.L. Kasner, S.J. Su, K. Patel, R. Cuellari, J. Phys. Chem. C 114 (2010) 14915–14921.
[18] J. Njagi, M.M. Chernov, J.C. Leiter, S. Andreescu, Anal. Chem. 82 (2010) 989–996.
[19] X.J. Qu, X.G. Liu, Y.H. Peng, S.Y. Ai, R.X. Han, X.B. Zhu, J. Electroanal. Chem. 654 (2011) 72–78.
[20] Y. Liu, J.S. Huang, H.Q. Hou, T.Y. You, Electrochem. Commun. 10 (2008) 1431–1434.
[21] K.S. Prasad, G. Muthuraman, J.M. Zen, Electrochem. Commun. 10 (2008) 559–563.
[22] L. Tan, K.G. Zhou, Y.H. Zhang, H.X. Wang, X.D. Wang, Y.F. Guo, H.L. Zhang, Electrochem. Commun. 12 (2010) 557–560.
[23] Y. Wang, Y.M. Li, L.H. Tang, J. Lu, J.H. Li, Electrochem. Commun. 11 (2009) 889–892.
[24] R. Yuan, Y. Zhang, Y.Q. Chai, W.J. Li, X. Zhong, H.A. Zhong, Biosens. Bioelectron. 26 (2011) 3977–3980.
[25] H.F. Cui, Y.H. Cui, Y.L. Sun, K. Zhang, W.D. Zhang, Nanotechnology 21 (2010) 215601–215608.
[26] J.P. Dong, Y.Y. Hu, S.M. Zhu, J.Q. Xu, Y.J. Xu, Anal. Bioanal. Chem. 396 (2010) 1755–1762.
[27] P.M. Ndangili, O.A. Arotiba, P.G.L. Baker, E.I. Iwuoha, J. Electroanal. Chem. 643 (2010) 77–81.
[28] J.S. Huang, Y. Liu, H.Q. Hou, T.Y. You, Biosens. Bioelectron. 24 (2008) 632–637.
[29] D. Zheng, J.S. Ye, L. Zhou, Y. Zhang, C.Z. Yu, J. Electroanal. Chem. 625 (2009) 82–87.
[30] C.L. Sun, H.H. Lee, J.M. Yang, C.C. Wu, Biosens. Bioelectron. 26 (2011) 3450–3455.
[31] S.A. Kumar, H.W. Cheng, S.M. Chen, Electroanalysis 21 (2009) 2281–2286.
[32] E.K. Wang, S.J. Guo, S.J. Dong, Adv. Mater. 22 (2010) 1269–1272.
[33] J.P. Li, J. Zhao, X.P. Wei, Sens. Actuators B 140 (2009) 663–669.
[34] L.P. Lu, S.Q. Wang, X.Q. Lin, Anal. Chim. Acta 519 (2004) 161–166.
[35] P.R. Solanki, N. Prabhakar, M.K. Pandey, B.D. Malhotra, Biomed. Microdevices 10 (2008) 757–767.
[36] G.F. Jie, B. Liu, H.C. Pan, J.J. Zhu, H.Y. Chen, Anal. Chem. 79 (2007) 5574–5581.
[37] Y. Liu, Y.Y. Yu, Q.Y. Yang, Y.H. Qu, Y.M. Liu, G.Y. Shi, L.T. Jin, Sens. Actuators B 131 (2008) 432–438.
[38] H.O. Finklea, D.A. Snider, J. Fedyk, E. Sabatani, Y. Gafni, I. Rubinstein, Langmuir 9 (1993) 3660–3667.
[39] Y.J. Yin, P. Wu, Y.F. Lu, P. Du, Y.M. Shi, C.X. Cai, J. Solid State Electrochem. 11 (2007) 390–397.
[40] J.J. Gooding, R. Wibowo, J.Q. Liu, W.R. Yang, D. Losic, S. Orbons, F.J. Mearns, J.G. Shapter, D.B. Hibbert, J. Am. Chem. Soc. 125 (2003) 9006–9007.
[41] J. Wang, Electroanalyis 17 (2005) 7–14.
[42] H.T. Deng, G.J. Van Berkel, Anal. Chem. 71 (1999) 4284–4293.
[43] Q.B. Fan, L.M. Ng, J. Vac. Sci. Technol. A 14 (1996) 1326–1329.
[44] Y.F. Zhao, Y.Q. Gao, D.P. Zhan, H. Liu, Q. Zhao, Y. Kou, Y.H. Shao, M.X. Li, Q.K. Zhuang, Z.W. Zhu, Talanta 66 (2005) 51–57.